Heat Mass Transfer (2011) 47:833–839
DOI 10.1007/s00231-010-0590-x

ORIGINAL

Experimental investigation of shell-and-tube heat exchanger with a new type of baffles

Yingshuang Wang · Zhichun Liu · Suyi Huang · Wei Liu · Weiwei Li

Received: 9 July 2009 / Accepted: 3 March 2010 / Published online: 24 February 2011

Abstract A shell-and-tube heat exchanger with new type of baffles, is designed, fabricated and tested. The experimental investigation for the proposed model and the original segmental baffle heat exchanger are conducted. The operation performances of the two heat exchangers are also compared. The results suggest that, under the same conditions, the overall performance of the new model is 20–30% more efficient than that of the segmental baffle heat exchanger.

1 Introduction

Heat exchanger is a very important apparatus in many fields, such as petroleum refining, power generation, chemical engineering, process industry, food industry, etc. Among the different types of heat exchangers, shell-and-tube heat exchanger (STHX) has many advantages such as reliable structure, mature techniques and wide applicability, which make it widely utilized in various industries [1]. The baffle element plays very important roles in STHX, such as supporting the tube bundles and disturbing the fluid of shell side. According the direction of fluid flow of shell side, the STHX can be divided into three groups: transverse flow, longitudinal flow and helical flow. The characteristics of pressure drop and heat transfer in shell side of the STHX vary under different flow states, which have a heavy impact on the performance of the heat exchangers.

Y. Wang · Z. Liu (✉) · S. Huang · W. Liu · W. Li
School of Energy and Power Engineering,
Huazhong University of Science and Technology,
Wuhan 430074, Hubei, People's Republic of China
e-mail: zcliu@mail.hust.edu.cn

The traditional shell-and-tube heat exchanger with segmental baffles (SB-STHX) have many disadvantages, such as high pressure drop, low heat transfer efficiency, harmful vibration caused by the shell-side flow which is normal to tube bundles. When the traditional segmental baffles are used in STHX, higher pumping power is often required to offset the higher pressure drop under the same heat load. Therefore, a new type of STHX using different types of baffles might achieve higher heat transfer efficiency and lower pressure drop. Pressure drop and heat transfer are two interdependent factors influencing the capital and operating costs of the heat exchange systems. In order to improve the performance, heat exchangers with different types of baffles are developed, which have relatively higher heat transfer efficiency and relatively lower pressure drop, such as rod baffles and helical baffle exchangers [2–11].

Therefore, the main objectives of this study are to develop an STHX with new type of baffles to overcome the deficiencies mentioned above and to experimentally investigate its performance. Moreover, performance of the new STHX is also compared with that of SB-STHX in this study.

2 Configuration and fabrication of the STHX with new type of baffles

The helical type of fluid flow in shell side of the STHX with helical baffles has led to some advantages such as high heat transfer efficiency and low flow resistance [5, 6, 8]. Nevertheless, it is difficult to manufacture the continuous helical baffles. In order to address this problem, flower baffles STHX (FB-STHX), a new type of STHX based on the traditional segmented baffle, is proposed in this paper and shown schematically as in Fig. 1. As seen in Fig. 1, a

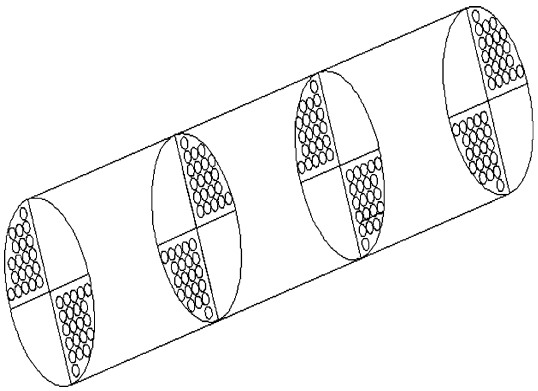

Fig. 1 Schema of the flower baffles arrangement

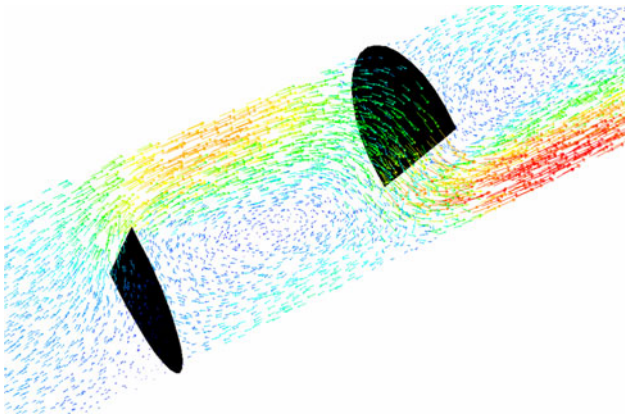

Fig. 2 Stream line for fluid flow over segmental baffles

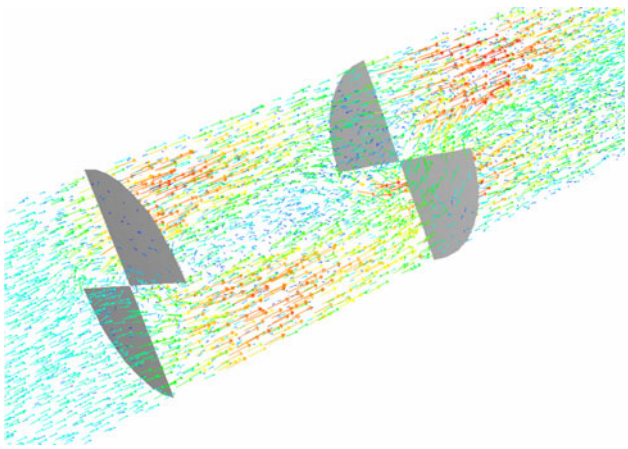

Fig. 3 Stream line for fluid flow over flower baffles

round baffle can be divided into four quadrants, and among the four quadrants, at least one quadrant is hollow for fluid flowing, and the remaining quadrants are used to support the heat tube. As the flower baffles are installed alternately, the phase angles (the angles for hollow parts of the two adjacent baffles) can be 30°, 60°, or 90°. Under different application situations, the phase angles may vary. From Fig. 1 it can also be observed that the configuration of all baffles in FB-STHX is the same; only the phase angles are different. As a result, the manufacturing process for the flower baffles is considerably simplified. The fabricating process of the flower baffles is the same as that of segment baffle, and the flower baffles are fixed by tension rods. In the present FB-STHX, there are four tension rods to fix the baffles. Figures 2 and 3 schematically show the stream line for the fluid flow over the segmental baffles and the flower baffles respectively. From the figures, it can be observed that the fluid flow in shell side for SB-STHX is zigzag and the fluid flow in shell side for FB-STHX is longitudinal with some swirling which will lead to some difference of heat transfer and flow resistance about these two type of STHXs. In this paper, the shell-side local heat transfer coefficients of FB-STHX were obtained experimentally and compared with that of SB-STHX.

The dimension of the heat exchanger is Φ159 mm × 5 mm. The detailed parameters of heat exchangers are shown in Tables 1 and 2.

Table 1 Structure parameter for FB-STHX

Shell side: Φ159 mm × 5 mm	Effective length of heat tube: 1,473 mm
Tube pass number: 2	Tube ID: 14.4 mm
Tube OD: 16 mm	Total number of tube: 24
Tube spacing: 20 mm	Diameter of tension rod: 12 mm
Number of tension rod: 4	Arranging style of tube: rectangle
Flow area of tube side: 0.0001953 m^2	Heat transfer area of tube outside: 1.777 m^2
Conductance for tube: 14.7 W/(m K)	Flower baffle spacing: 170 mm
Minimum flow area for shell side: 0.0061 m^2	

Table 2 Structure parameter of SB-STHX

Shell side: Φ159 mm × 5 mm	
Effective length of tube: 1,473 mm	Tube pass number: 2
Tube OD: 16 mm	Tube ID: 14.4 mm
Tube spacing: 20 mm	Tube total number: 24
Number of tension rod: 4	Diameter of tension rod: 12 mm
Arranging style for tubes: triangle	
Flow area in tube side: 0.0001953 m^2	Heat transfer area of tube outside: 1.777 m^2
Conductance of tube wall: 14.7 W/(m K)	Baffle spacing: 148 mm
Minimum flow area in shell side: 0.0098 m^2	

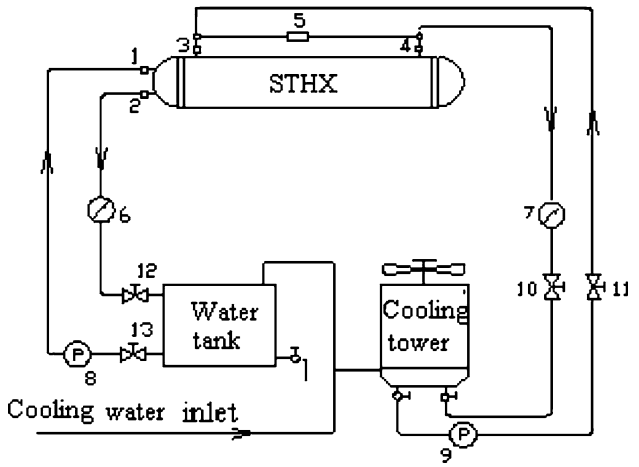

Fig. 4 Schema of experimental system. *1*, *2*, *3*, *4* Thermal couple; *5* differential pressure transducer; *6*, *7* flowmeter; *8*, *9* pump; *10*, *11*, *12*, *13* value

3 Experimental devices and approaches

The experimental system for studying the heat transfer and pressure drop for STHX is schematically shown in Fig. 4. The experiment setup consists of two loops: hot water loop and cold water loop. The detailed descriptions of the two loops are given below.

(1) *Hot water loop* In this loop, water is heated by an electrical heater with a temperature controlling device. The hot water flows from a water tank via a tube into the tube side of the STHX. After transferring the heat to fluid of shell side, the water flows from the STHX to a volumetric flowmeter (6) and finally returns to the water tank. The inlet and outlet temperatures of the heated water flowing through the STHX are measured by thermocouples (1) and (2), respectively. The hot water is cycled by a pump (8). The valves (12) and (13) are used to regulate the flow rates.

(2) *Cold water loop* In this loop, water is cooled by a cooling tower. The cold water flows from a water tank via a tube into the shell side of the STHX. After absorbing the heat from the fluid of the tube side, the water flows from the STHX into a volumetric flowmeter (7) and finally returns to the water tank. The inlet and outlet temperatures of the cold water flowing through the STHX are measured by thermocouples (3) and (4) respectively. The cold water is recycled by a pump (9). The valves (10) and (11) are used to regulate the flow rate.

A water replenishing device is utilized to supplement the water loss for both the hot water side and the cold water side.

4 Data acquisitions

In the experiments, the flow rate, temperature, and pressure drop were measured. The energy imbalance between the shell side and the tube side was calculated from the data on the flow rates, and the inlet and the outlet temperatures both in shell and tube sides. The heat balance was considered to be achieved when the energy imbalance is less than 5%. Based on the energy balance between the shell and tube side, the overall heat transfer coefficient of the STHX can be calculated. The tube side heat transfer coefficient can be calculated using the classical correlation, so the shell side heat transfer coefficient can be obtained using the overall heat transfer calculation correlation. The overall pressure drop can be directly measured. So the correlation between the friction factor f, Nusselt number Nu and Reynolds Re can be obtained. The detailed procedures are presented as follows.

The overall heat transfer coefficient for heat exchangers can be computed using Eq. 1 [12]

$$k = \frac{1}{\frac{1}{h_i}\frac{d_o}{d_i} + R_i + R_w + R_o + \frac{1}{h_o}} \tag{1}$$

where h_i, heat transfer coefficient for tube side, W/(m^2 K); h_o, heat transfer coefficient for shell side, W/(m^2 K); R_i, fouling coefficient for tube side, (m^2 K)/W; R_o, fouling coefficient for shell side, (m^2 K)/W; R_w, thermal resistance for tube wall, (m^2 K)/W.

Since the heat exchangers in our experiments are newly fabricated, the effects of the two fouling resistance are negligible. Therefore, the above equation can be expressed as

$$k = \frac{1}{\frac{1}{h_i}\frac{d_o}{d_i} + R_w + \frac{1}{h_o}} \tag{2}$$

Based on the transfer correlation, the overall heat transfer coefficient can be achieved as

$$k = \frac{Q}{A \cdot \Delta t_m} \tag{3}$$

where Q, the average heat flux between the cold and the hot fluid, W; A, heat transfer area based on the tube out diameter, m^2, which can be calculated using Eq. 4.

$$A = n\pi d_o L \tag{4}$$

N, tube number; d_o, tube out diameter, m; L, effective length of tube, m; Δt_m, logarithm averaged temperature for the cold and the hot fluid, °C

The heat exchanger is double tube passes and one shell pass, and the logarithm averaged temperature difference can be stated as [12]

$$\Delta t_m = \frac{(t_2'' - t_2')\sqrt{R^2+1}}{\ln\frac{2-P(1+R-\sqrt{R^2+1})}{2-P(1+R+\sqrt{R^2+1})}} \tag{5}$$

where $R = \frac{t_1' - t_1''}{t_2'' - t_2'}$, $P = \frac{t_2'' - t_2'}{t_1' - t_2'}$; t_1', t_1'', in and out temperature for tube side fluid, °C; t_2', t_2'', in and out temperature for shell side fluid, °C.

Heat transfer between cold and hot fluid can be achieved according to following equation

$$Q = \dot{m} \cdot c_p \cdot \Delta t \tag{6}$$

$\dot{m}$, fluid mass flowrate, kg/s; c_p, specific heat under constant pressure, J/(kg K).

According to Eqs. 2–5, the overall heat transfer coefficient can be obtained.

Heat transfer performance on the tube side can be obtained by the following equation [13]

$$Nu = 0.027 Re_{\mathrm{f}}^{0.8} Pr_f^{1/3} \left(\frac{\eta_f}{\eta_w}\right)^{0.14} \tag{7}$$

Subscript f indicates the fluid temperature, and w indicates the wall temperature.

The thermal resistance of tube wall can be obtained by

$$R_w = \frac{d_o}{2\lambda} \ln \frac{d_o}{d_i} \tag{8}$$

The tube material is chrome nickel steel and the its conductance λ is 14.7 W/(m K).

After computing the heat transfer coefficient in tube side and thermal resistance for tube wall according Eqs. 6 and 7, and substituting them and the total heat transfer coefficient k into Eq. 1, we can get the heat transfer coefficient h_o of shell side.

The Nu, f, and Re are defined as follows:

$$Nu = \frac{h_o d_o}{\lambda_f} \tag{9}$$

$$f = \frac{\Delta p_o}{(1/2)\rho u^2} \frac{d_o}{l} \tag{10}$$

$$Re = \frac{\rho u d_o}{\mu_f} \tag{11}$$

where Δp_o is the overall pressure drop on the shell side of the STHX, l is the effective length of tubes, d_o is the outer diameter of the tube.

5 Experimental results and analysis

The experiments were conducted for the two types of STHXs described in Sect. 2, in which hot water flowed on the tube side and cold water flowed on the shell side of the STHXs. In order to verify the reliability of the experiment results, the heat transfer and fluid flow characteristics under three different tube inlet velocities (0.70, 0.94 and 1.2 m/s) for SB-STHX and FB-STHX are investigated. And performances

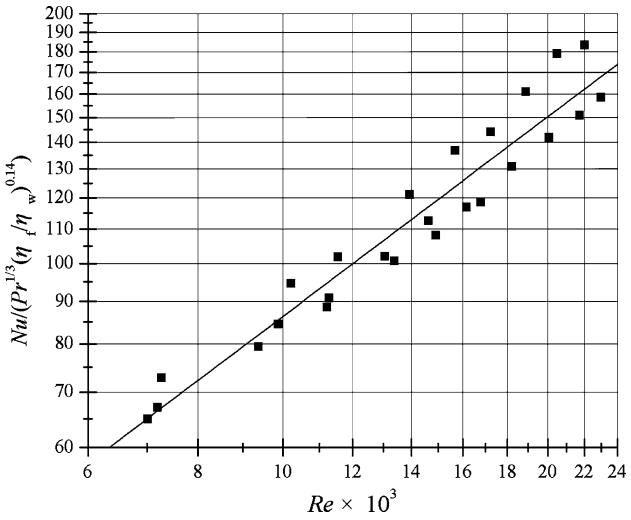

Fig. 5 Heat transfer correlation for FB-STHX

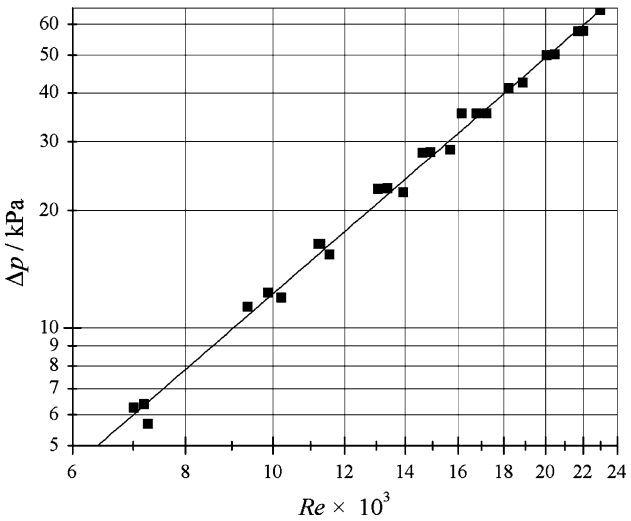

Fig. 6 Flow resistance correlation for FB-STHX

between the above two exchanger are compared. Proper evaluation is important for comparing the comprehensive performance of different heat exchangers. Both heat transfer coefficient and pressure drop are important parameters for performance evaluation of heat exchangers. It is desirable to obtain the highest heat transfer rate at the lowest pressure drop, so the ratio of Nusselt number Nu to pressure drop is used as a comparison criterion in the present study.

Figures 5 and 6 show the heat transfer correlation and flow resistance correlation for FB-STHX under the above three tube side inlet velocities. In the figures, the lines shown in these figures were fitted by the method of least squares, and the heat transfer correlation in the range of $7{,}000 \leq Re \leq 23{,}000$ can be expressed as Eq. 12 and the correlation coefficient is $r = 0.9645$.

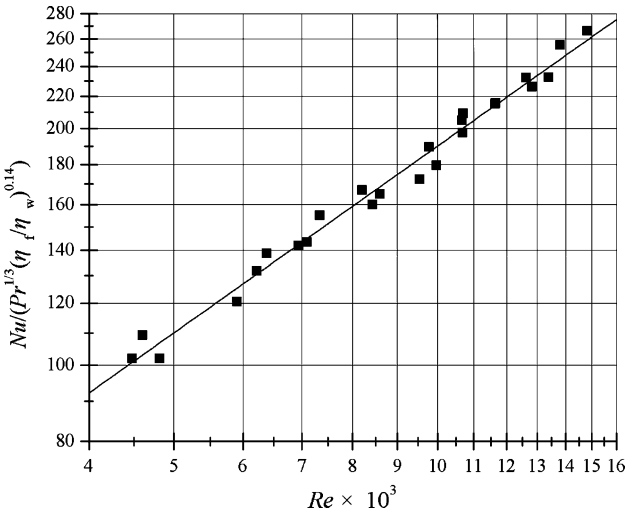

Fig. 7 Heat transfer correlation for SB-STHX

$$Nu = 0.0548 Re_f^{0.7994} Pr_f^{1/3} \left(\frac{\eta_f}{\eta_w}\right)^{0.14} \quad (12)$$

The flow resistance correlation in the ranger of $7{,}000 \leq Re \leq 23{,}000$ can be expressed as Eqs. 13–14 and the correlation coefficient for above equation is $r = 0.9957$.

$$\Delta p = 1.1523 \times 10^{-7} Re_f^{2.0067} \quad (13)$$

$$f = 0.1613 Re_f^{-0.0284} \quad (14)$$

It can be seen from Figs. 5 and 6, that the Nusselt number Nu and pressure drop will increase with the increase of Re number, and under the same shell side velocity and with different tube velocities for FB-STHX the heat transfer and flow resistance characteristic in shell side are almost the same, which prove the good repetition of the experiments.

Figures 7 and 8 show the heat transfer and flow resistance characteristics for SB-STHX. The lines shown in these figures were fitted by the method of least squares, and the heat transfer correlation in the range of $4{,}000 \leq Re \leq 15{,}000$ can be expressed as Eq. 15 and the correlation coefficient for above equation is $r = 0.9929$.

$$Nu = 0.1328 Re_f^{0.7889} Pr_f^{1/3} \left(\frac{\eta_f}{\eta_w}\right)^{0.14} \quad (15)$$

The flow resistance correlation in the ranger of $4{,}000 \leq Re \leq 15{,}000$ can be expressed as Eqs. 16–17 and the correlation coefficients are $r = 0.9983$, $r = 0.9988$ respectively.

$$\Delta p = 4.7475 \times 10^{-7} Re_f^{1.9957} \quad (16)$$

$$f = 0.7850 Re_f^{-0.0566} \quad (17)$$

As shown in Figs. 7 and 8, the Nusselt number Nu and pressure drop will increase with the increase of Re number.

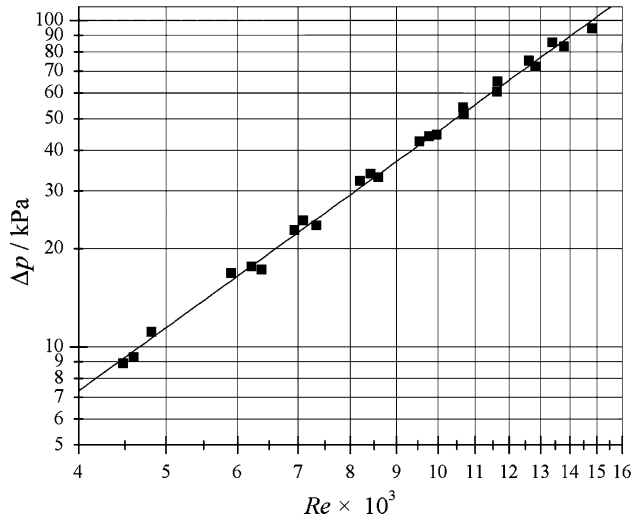

Fig. 8 Flow resistance correlation for SB-STHX

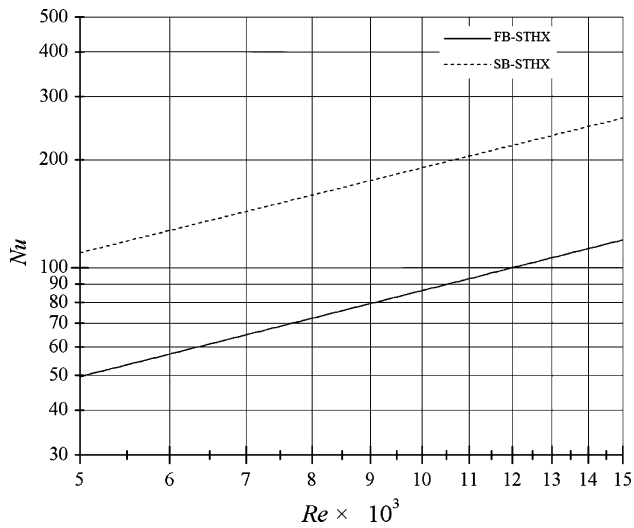

Fig. 9 Comparison of Nu number between FB-STHX and SB-STHX

Under the same shell side velocity and with different tube velocity for SB-STHX the heat transfer and flow resistance characteristic are almost same, which prove the good repetition of the experiments.

The comparison of Nu number and pressure drop Δp in shell side between FB-STHX and SB-STHX can be seen in Figs. 9 and 10. Nusselt number Nu increases with the increase of Reynolds number Re for the two heat exchangers, and the pressure drop increases with the increase of the Reynolds number Re for both heat exchangers. From the figures it can be observed that, with same Re number, the Nu number of FB-STHX is about 50% of that of SB-STHX, but the pressure drop Δp of the former is only 30% of that of the latter. This is because the fluid flow in shell side of flower baffle heat exchanger is

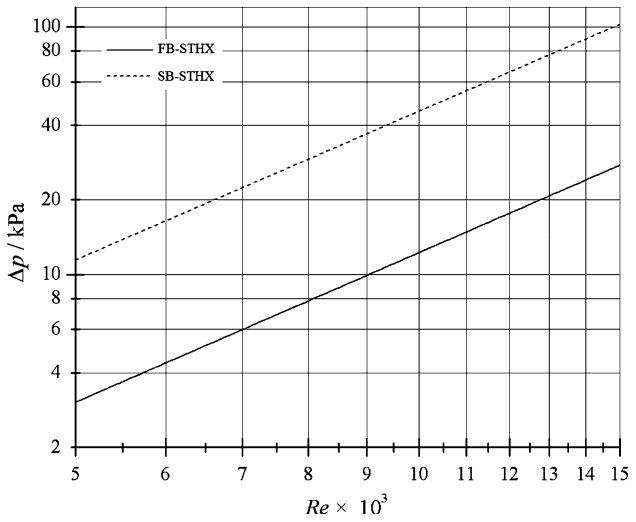

Fig. 10 Comparison of pressure drop Δp number between FB-STHX and SB-STHX

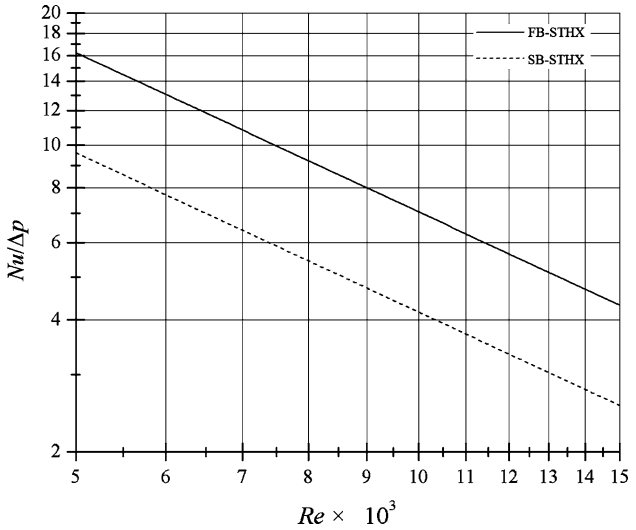

Fig. 11 Comparison of the comprehensive performance drop $Nu/\Delta p$ between FB-STHX and SB-STHX

longitudinal, but the fluid flow in shell side of segmental baffle heat exchanger is transverse. As a result, the heat transfer of the flower baffle heat exchanger is less than that of the segmental baffle heat exchanger. Because of this, the pressure drop in shell side of flower baffle is also less than that of the segmental baffle heat exchanger.

Figure 11 shows the comprehensive comparison of performance $Nu/\Delta p$ between FB-STHX and SB-STHX. With same Re number, the comprehensive performance $Nu/\Delta p$ of FB-STHX is about 60% higher than that of SB-STHX.

To sum up, in the same shell side Re, the shell side Nu of FB-STHX is less than that of the SB-STHX, and the pressure drop of the former is also less than that of the latter, but the decreasing amplitude of the flow resistance is larger than that of the heat transfer. As a result, the comprehensive performance $Nu/\Delta p$ of FB-STHX is higher than that of the SB-STHX. Therefore, it could be concluded that with same pressure drop, the Nu number of the FB-STHX is higher than that of the SB-STHX.

6 Experimental uncertainty analysis

The experimental uncertainty of the present work is determined by using the method presented by Ref. [14]. The uncertainty calculation method involves calculating derivatives of the desired variable with respect to individual experimental quantities and applying known uncertainties. According to Ref. [14], the experimental uncertainty is defined as follow:

$$W_R = \sqrt{\left(\frac{\partial R}{\partial x_1} W_{x_1}\right)^2 + \left(\frac{\partial R}{\partial x_2} W_{x_2}\right)^2 + \cdots + \left(\frac{\partial R}{\partial x_n} W_{x_n}\right)^2} \tag{18}$$

where $R = f(x_1, x_2, \ldots, x_n)$, $x_1, x_2, \ldots, x_n$ are the variables that affect the results of R, $w_{x_1}, w_{x_2}, \ldots, w_{x_n}$ are the absolute uncertainties of $x_1, x_2, \ldots, x_n$.

The uncertainties involved in the friction factors for FB-STHX and SB-STHX are ±3.6 and ±4.2%, respectively, and the uncertainties involved in the Nu number for FB-STHX and SB-STHX are within ±7.8 and ±8.1%, respectively.

7 Conclusion

The characteristics of heat transfer and flow resistance for the FB-STHX and the SB-STHX have been experimentally investigated. And performance comparisons between the FB-STHX and the SB-STHX are conducted. The heat transfer and flow resistance correlation for SB-STHX and FB-STHX were developed based on the experiment results. The experimental results showed that under circumstance of the same Re number both in shell and tube side, the Nusselt number Nu for FB-STHX is about 50% of that of SB-STHX while the pressure drop of the former is about 30% of the latter. But the comprehensive performance $Nu/\Delta p$ of the former is 60% higher than that of the latter. For the sake of energy saving in designing heat exchangers, both heat transfer enhancement and flow resistance increase should be taken into consideration. By properly designing FB-STHX the heat transfer and pressure drop performance can be improved relative to the traditional SG-STHX.

Acknowledgments This work was supported by the National Key Basic Research Development Program of China (Grant No. 2007CB206903) and the Natural Science Foundation of China (Grant No. 51036003). Mr. Ho Simon Wang at HUST Academic Writing Center has helped improve the linguistic presentation of this paper.

References

1. Qian SW (2002) Handbook for heat exchanger design. Chemical Industry Press, Beijing (in Chinese)
2. Mukherjee R (1992) Use double-segmental baffles in the shell-and-tube heat exchangers. Chem Eng Prog 88:47–52
3. Li H, Kottke V (1999) Analysis of local shell side heat and mass transfer in the shell-and-tube heat exchanger with disc-and-doughnut. Int J Heat Mass Transf 42:3509–3521
4. Li H, Kottke V (1998) Effect of baffle spacing on pressure drop and local heat transfer in shell-and-tube heat exchangers for staggered tube arrangement. Int J Heat Mass Transf 41(10):1303–1311
5. Lei YG, He YL, Rui L et al (2008) Effects of baffle inclination angle on flow and heat transfer of a heat exchanger with helical baffles. Chem Eng Process 47(12):2336–2345
6. Lei YG, He YL, Pan C et al (2008) Design and optimization of heat exchangers with helical baffles. Chem Eng Sci 63(17):4386–4395
7. Dong QW, Wang YQ, Liu MS (2008) Numerical and experimental investigation of shell side characteristics for rod baffle heat exchanger. Appl Therm Eng 28:651–660
8. Peng B, Wang QW, Zhang C et al (2007) An experimental study of shell-and-tube heat exchangers with continuous helical baffles. J Heat Transf 129:1425–1431
9. Kara YA, Guraras OA (2004) Computer program for designing of shell-and-tube heat exchangers. Appl Therm Eng 24:1797–1805
10. Costa André LH, Queiroz Eduardo M (2008) Design optimization of shell-and-tube heat exchangers. Appl Therm Eng 28(14–15): 1798–1805
11. Xie GN, Wang QW, Zeng M et al (2007) Heat transfer analysis for shell-and-tube heat exchangers with experimental data by artificial neural networks approach. Appl Therm Eng 27:1096–1104
12. Bejan A, Kraus AD (2003) Heat transfer handbook. Wiley, New Jersey
13. Holman JP (1997) Heat transfer. McGraw-Hill, New York
14. Wheeler AJ, Ganji AR (2004) Introduction to engineering, 2nd edn. Prentice-Hall, Englewood Cliffs